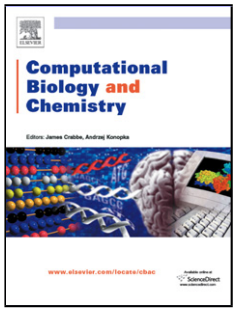

Title: In silico characterization of the interaction between LSKL peptide, a LAP-TGF-beta derived peptide, and ADAMTS1

Author: Marie-Amandine Laurent Dominique Bonnier Nathalie Théret Pierre Tufféry Gautier Moroy

PII: S1476-9271(16)30054-8
DOI: http://dx.doi.org/doi:10.1016/j.compbiolchem.2016.01.012
Reference: CBAC 6506

To appear in: *Computational Biology and Chemistry*

Received date: 2-3-2015
Revised date: 28-1-2016
Accepted date: 28-1-2016

Please cite this article as: Laurent, Marie-Amandine, Bonnier, Dominique, Théret, Nathalie, Tufféry, Pierre, Moroy, Gautier, In silico characterization of the interaction between LSKL peptide, a LAP-TGF-beta derived peptide, and ADAMTS1.Computational Biology and Chemistry http://dx.doi.org/10.1016/j.compbiolchem.2016.01.012

In silico characterization of the interaction between LSKL peptide, a LAP-TGF-beta derived peptide, and ADAMTS1.

Running title: *In silico* characterization of LSKL-ADAMTS1 interaction.

Marie-Amandine Laurent[1], Dominique Bonnier[2], Nathalie Théret[2], Pierre Tufféry[1], Gautier Moroy[1*]

[1]Université Paris Diderot, Sorbonne Paris Cité, Molécules Thérapeutiques *in silico* (MT*i*), Inserm UMR-S 973, 35 rue Hélène Brion, 75013 Paris, France.

[2]INSERM U1085, Institut de Recherche en Santé, Environnement et Travail (IRSET), Université de Rennes 1, 2 avenue Pr Léon Bernard, Rennes, France.

[*]Corresponding author: Tel.: +331 57278385; Fax: +331 57278372; Email: gautier.moroy@univ-paris-diderot.fr

Graphical abstract

Binding mode of LSKL peptide, in cyan, with ADAMTS1, in wheat color. The nonbonded interactions are represented in yellow dashed lines. The binding sequence of ADAMTS1 is colored in red.

Highlights

- We have experimentally shown that TSP-1 domain of ADAMTS1 is able to bind TGF-β.
- Docking experiments confirm that KTFR sequence interacts with LSKL peptide.
- MD simulations reach a stable binding mode between TSP-1 domain and LSKL peptide.

Abstract

Metalloproteases involved in extracellular matrix remodeling play a pivotal role in cell response by regulating the bioavailability of cytokines and growth factors. Recently, the disintegrin and metalloprotease, ADAMTS1 has been demonstrated to be able to activate the transforming growth factor TGF-β, a major factor in fibrosis and cancer. The KTFR sequence from ADAMTS1 is responsible for the interaction with the LSKL peptide from the latent form of TGF-β, leading to its activation. While the atomic details of the interaction site can be the basis of the rational design of efficient inhibitory molecules, the binding mode of interaction is totally unknown.

In this study, we show that recombinant fragments of human ADAMTS1 containing KTFR sequence keep the ability to bind the latent form of TGF-β. The recombinant fragment with the best affinity is modeled to investigate the binding mode of LSKL peptide with ADAMTS1 at the atomic level. Using a combined approach with molecular docking and multiple independent molecular dynamics (MD) simulations, we provide the binding mode of LSKL peptide with ADAMTS1. The MD simulations starting with the two lowest energy model predicted by molecular docking shows stable interactions characterized by 3 salt bridges (K_3-

NH_3^+ with E_{626}-COO^- ; L_4-COO^- with K_{619}-NH_3^+ ; L_1-NH_3^+ with E_{624}-COO^-) and 2 hydrogen bonds (S_2-OH with E_{623}-COO^- ; L_4-NH with E_{623}-COO^-). The knowledge of this interaction mechanism paves the way to the design of more potent and more specific inhibitors against the inappropriate activation of TGF-β by ADAMTS1 in liver diseases.

List of abbreviations: ADAM, a disintegrin and metalloproteinase; ADAMTS, ADAM with thrombospondin domains motifs; ECM, extracellular matrix; LAP, latency-associated protein; LGA, Lamarckian genetic algorithm; K_d, dissociation constant ; MD, molecular dynamics ; RMSD, root mean-square deviation; SLC, small latent complex; TGF-β = transforming growth factor-β; TSP1, thrombospondin type-1

Keywords: ADAMTS1; extracellular matrix; hepatic fibrosis, molecular dynamics simulation; TGF-beta peptide.

Introduction

The extracellular matrix (ECM) is the complex environment surrounding the cells in solid tissue. The ECM remodeling by metalloproteases is required for physiological events such as morphogenesis, development or tissue repair. However, alterations in expression and activities of these proteases are implicated in many diseases such as fibrosis and cancers [1].

Metalloproteases belonging to the ADAM (a disintegrin and metalloproteinase) protein family are characterized by a multi-domain organization that includes metalloprotease, disintegrin, cystein, transmembrane and cytoplasmic domains and are involved in ectodomain shedding, cell adhesion and cell signaling. While ADAMs are highly expressed in cancer cells and tissues, their functions are not still precisely understood [2].

ADAMTS (ADAM with thrombospondin motifs) members are secreted-type ADAMs that associate with ECM components and are characterized by the presence of one or more thrombospondin type-1 repeats (TSP1). The ADAMTS1 gene was originally cloned from a colon carcinoma cell line and ADAMTS1 upregulation is associated with cell proliferation, inhibition of apoptosis and altered vascularization [3]. ADAMTS1 has been firstly described as a protease, which degrades mainly proteoglycans, such as aggrecan and versican. However, we have recently demonstrated a new proteolytic-independent role in liver fibrosis demonstrating that ADAMTS1 induces the activation of the transforming growth factor-β (TGF-β) [4].

TGF-β is one of the most important regulators of tissue homeostasis and upregulation and activation of TGF-β has been linked to various diseases, including fibrosis and cancer through promotion of cell proliferation and invasion and of the epithelial-mesenchymal transition [5]. To antagonize the increase TGF-β activity in diseases, many strategies have been developed including ligand traps, small inhibitory molecules and antisense based approaches [6], however

more specific targeting method are required to take into account the pathological activity of TGF-β.

TGF-β is synthesized as an inactive homodimeric large precursor molecule consisting of a self-inhibiting propeptide, the latency-associated protein (LAP), in addition to the covalently linked active form of TGF-β. Pro-TGF-β is then intracellularly cleaved by furin-type enzymes to generate mature TGF-β which remains non-covalently associated with LAP as the small latent complex (SLC). TGF-β, secreted as SLC, cannot bind to its cell surface receptors and the release of biologically active TGF-β requires its dissociation from LAP in a process termed latent TGF-β activation. Numerous protease- and non protease-dependent mechanisms, which differ according to cell type and to the physiological context, have been implicated in the conversion of latent TGF-β into its biologically active form, *i.e.* dissociation of TGF-β from LAP-TGF-β in the soluble SLC and/or from the ECM-bound SLC [7]. Interestingly, we have recently demonstrated that ADAMTS1 binds LAP-TGF-β and induces the release of active TGF-β [4].

The TGF-β activation occurs through the interaction between a KTFR sequence of ADAMTS1 and a LSKL sequence of TGF-β [4]. The KTFR motif is localized in ADAMTS1 cysteine-rich domain and the LSKL sequence in LAP subunit of latent TGF-β. Interestingly, LSKL peptide is able to reduce liver fibrosis by inhibiting TGF-β activation. To note, LSKL peptide has been shown to have an equivalent effect on liver fibrosis in rats [8].

The knowledge of the binding mode of a targeted protein with a partner is often the cornerstone of the rational design of new therapeutic molecule. In this paper, the ability of two recombinant fragments of human ADAMTS1, containing the KTFR sequence, to bind LAP-TGF-β was assessed experimentally. Then, we have characterized the binding mode of LSKL peptide on the greater recombinant fragment of ADAMTS1, called F1, using molecular modeling methods. LSKL peptide was docked at ADAMTS1 surface and the stability of binding modes was investigated by multiple molecular dynamics (MD) simulations.

Methods and Materials

Preparation of recombinant fragments and binding experiments

Recombinant fragments of human ADAMTS1 containing KTFR sequence, called F1 (from F_{554} to F_{849}, 33 kDa) and F2 (from F_{554} to K_{725}, 19 kDa) were produced as previously described [9]. While F1 is composed of TSP1-1 domain, the spacer domain and the cysteine-rich domain, F2 is only formed by TSP1-1 domain and the spacer domain.

Affinity measurements were performed using MicroScale Thermophoresis technology with a Nanotemper Monolith NT.115 (Nanotemper, Munich, Germany) and standard treated capillaries. Settings were: Red excitation and detection, 50% LED, 40% MST power and 25°C temperature control setting. LAP-TGF-β (Biosciences, Cambridge, UK) was labeled using the Monolith NT Protein Labeling Kit RED (NanoTemper Technologies) according to the supplied

protocol. The concentration of labeled LAP-TGF-β was kept constant at 62.5 nM. The corresponding unlabeled binding partners (F1 and F2) were titrated in 1:10 dilutions. As positive control, we use thrombospondin-1, the well-known interactant of LAP-TGF-β.

Structures

LSKL peptide was built in a fully extended model with N and C extremities charged, using c35b4 version of CHARMM program [10-11].

The ADAMTS1 structure at the atomic level is not available in the Protein Data Bank [12-13]. However, a homology model of the F2 recombinant fragment, containing the TSP1-1 domain, the spacer domain and the cysteine-rich domain, has been previously built [4]. The sequence identity between the selected domains of the human ADAMTS1 sequence and the sequences of the related proteins structures (ADAMTS13, ADAMTS5 and proteins with TSP1-1 domain) is of 30.4 %. The structure of the model is stabilized by 8 disulfide bonds (3 in TSP1-1 domain and 5 in cysteine-rich domain), which are conserved between related proteins structures and ADAMTS1. Molecular dynamics (MD) simulations have been performed for over 12 ns to assess the stability of the model. The MD analysis has been shown a conformational stability of the region encompassing the KTFR motif and a preservation of its solvent exposure. KTFR sequence is in α-helical structure, which is a very stable structure, generally well-predicted and well-built using homology modeling approaches. K, T and F residues are exposed to the solvent and able to interact with a partner, in accordance with experimental results. R residue is buried due to its interaction with other parts of ADAMTS1. The protonation states of titratable residues have been calculated at physiological pH of 7.0, using PROPKA program [14].

Molecular docking

The molecular docking computations attempt to predict the structure of a complex formed between a ligand and a targeted protein. In the case of short peptides, classical molecular docking programs, such as AutoDock program [15-16] or Glide program [17], that have been developed for the docking of small molecules have been proven to be efficient.

The molecular docking has been carried out using AutoDock 4.2 program [18-19]. Gasteiger partial charges for both ADAMTS1 and LSKL peptide as well the generation of the input files necessary to the docking procedures have been performed using the AutoDockTools package. At first, docking computations have been done on the whole ADAMTS1 surface to verify whether AutoDock is able or not to find the expected binding site for the interaction, *i.e.* KTFR sequence. The grid box size for this "blind docking" procedure was set to 126 x 126 x 126 points with a grid spacing of 0.70 Å. Such spacing between the grid points is not sufficiently precise to provide accurate models at the atomic level. For the regions of interest identified

during the blind docking, a narrower grid has been employed. This second grid box was centered on the position obtained previously during the "blind docking" step. The grid dimensions were set of 126 x 126 x 126 points with a spacing of 0.22 Å. We have employed the Lamarckian genetic algorithm (LGA) for ligand conformational searching. Four independent runs of docking computations have been done with, for each, the following parameters: 250 LGA operations, a population size of 250 individuals, a maximum of 2 000 000 energy evaluations and a maximum of 2 700 generations. The default parameters for Solis and Wet local search were used. During the docking computations, all the torsion angles of the LSKL peptide were allowed to be rotatable, except the ϖ dihedral angles of the peptide bonds, which were fixed to 180°.

The two lowest energy models obtained with the precise grids were selected. Afterwards, the stability of these models of interaction has been evaluated by MD simulations.

Molecular dynamics simulations

MD simulations were performed at 300 K with the CHARMM program [10-11], version c35b4 and the CMAP correction [20-21]. We employed the FACTS [22] implicit solvent model, which is based on generalized Born approach. Nonbonded interactions were truncated in a cut-off distance of 12 Å with a shift function for electrostatics and a switch function for the van der Waals terms. SHAKE [23] was applied to covalent bonds involving hydrogen. The "leapfrog" Verlet algorithm and an integration time step of 2 fs were used to solve the equations of motion. The studied systems were composed by LSKL peptide in interaction with ADAMTS1. The starting positions and conformations of LSKL peptide were those deriving from the docking computations. During all the steps of the MD simulations, no constraint was applied to maintain the binding mode. The entire system was minimized with 500 steps of steepest descent followed by 500 steps of conjugate gradient. The system was gradually heated during 200 ps to reach 300 K and then equilibrated during 400 ps with a temperature window of 300±10 K. For each of the two binding modes selected after the docking computations, three MD simulations of 12 ns were performed with different initial velocities. To increase the conformational sampling, these MD were extended up to 22 ns. Moreover, for the lowest energy model, six additional MD simulations of 12 ns were done with different initial velocities so as to further assess the stability of the complex. The dynamical behavior of the cysteine-rich domain structure was evaluated during the MD simulations by the calculation of the root mean-square deviation (RMSD) with respect of the starting structure (Figure S1). Along the trajectories, the RMSD is globally stable with only low fluctuations, indicating that stable structures have been reached and structural analysis can be done.

Results

Experimental binding experiments:

The activation of LAP-TGF-β by thrombospondin-1 is well-known and has been employed to be the positive control of our measurements. The experimental dissociation constant K_d for this interaction is measured to 0.15 µM (Figure 1A). Concerning the interaction between LAP-TGF-β and F1 or F2, the K_d are 2.85 µM and 11.1 µM respectively. As it was expected, the recombinant fragments containing the KTFR domain conserve the ability to bind LAP-TGF-β. Interestingly, the presence of the cysteine-rich domain seems induce a better affinity for LAP-TGF-β, which suggests a better stability of the recombinant fragment structure containing this domain. Therefore, we will use this F1 recombinant fragment for the following experiments in order to characterize the binding mode of LSKL peptide with ADAMTS1.

Binding site / binding mode:

The blind docking experiments have been performed to identify the most likely binding site for LSKL peptide on the ADAMTS1 surface. In accordance with experimental data, the lowest energy models calculated by AutoDock program are localized in contact with KTFR sequence (Figure 2A).

Further docking computations, centered on the KTFR sequence, have therefore been done. In docking experiments, it is frequent that only the lowest energy model is considered as the more realistic binding mode. However, since the AutoDock scoring function has been calibrated for small ligands, we have taken into account the two lowest energy models for the binding mode analysis. These are called hereafter, pose 1 and pose 2, respectively.

Pose 1 (Figure 2B) corresponds to the lowest energy model. It is characterized by van der Waals contacts between $L_1S_2L_3$ and $K_{619}T_{620}$, three salt bridges (the N-terminal extremity of LSKL peptide with the carboxylate group of E_{627}; the ammonium group of K_3 with the carboxylate group of $E_{644;}$ the C-terminal extremity of LSKL peptide and the ammonium group of K_{665}) and two hydrogen bonds (hydroxyl group of S_2 with the carboxylate group of E_{623}; the backbone amino group of K_3 with the carboxylate group of E_{623}).

Pose 2 (Figure 2C) binds to ADAMTS1 in a slightly different position than the pose 1. The LSKL peptide is closer to KTFR sequence. While in the lowest energy model T_{620} is partially exposed to the solvent, T_{620} is completely buried by the peptide in the second model. Van der Waals contacts are mostly observed between $L_1K_3L_4$ and $K_{619}T_{620}$. Moreover, three hydrogen bonds stabilize the interaction between the N-terminal extremity of LSKL peptide and the carboxylate group of E_{624} and between the ammonium group of K_3 of LSKL peptide and both the carboxylate group of E_{623} and the carboxylate group of $E_{627.}$

These two binding modes seem plausible; pose 1 exhibits more non-bonded interactions, whereas pose 2 has a higher contact surface with the binding sequence.

The binding modes investigated by MD simulations:

We now turn to the analysis of the three independent MD simulations of 12 ns – noted MD 1, MD 2 and MD 3 - carried out with different initial velocities to study the stability of pose 1. Figure 3A shows the evolution of the distance between the mass center of LSKL peptide and the mass center of KTFR sequence along trajectories. It allows to evaluate the position of LSKL peptide at ADAMTS1 surface. In MD 1 and MD 3, the distance appears stable around 8 Å, suggesting that the peptide has converged to a position close to KTFR sequence. A change in the position of LSKL peptide occurs at the beginning of the MD 1 and MD 3, after what the associated binding mode is conserved during the entire trajectory, except for some transient structures. This pose (Figure 4A and 4B) is characterized by van de Waals contacts between $L_1S_2K_3$ and $K_{619}T_{620}$. The rearrangement of LSKL peptide corresponds to the breaking of the 3 salt bridges with concomitant formation of two new salt bridges between the ammonium group of K_3 and the carboxylate group of E_{627} and between C-terminal extremity of LSKL peptide and the ammonium group of K_{619}. Moreover, only in MD 3, a third salt bridge is observable between N-terminal extremity of LSKL peptide and the carboxylate group of E_{624}. In the MD 1, the distance between these two atoms is too far away, around 6 Å, to form a salt bridge. The hydrogen bond, initially present, between hydroxyl group of S_2 and the carboxylate group of E_{623} is conserved during these two MD simulations. Furthermore, the backbone amino group of L_4 is involved in a stable hydrogen bond with the carboxylate group of E_{623}.

On the contrary, during MD 2, the peptide drifts away from KTFR sequence, with a mean distance around 15 Å (Figure 3A) and it does no longer interact with KTFR sequence. This result is interesting because it means that the employed protocol did not impose the conservation of the starting structure, but allows a sufficient freedom to explore the potential energy surface of the studied system.

The three MD were prolonged up to 22 ns to confirm the stability of the binding mode detected during the MD 1 and MD 3. Along the trajectories, the distance between the mass center of LSKL peptide and the mass center of KTFR sequence has a constant value of 8 Å for the MD 1 and MD 3 (Figure S2), clearly indicating that this binding mode is stable. Moreover, in the MD 1, a change in orientation of the side chain of L_1 was occurred after about 15 ns, inducing the formation of the same salt bridge (between N-terminal extremity of LSKL peptide and the carboxylate group of E_{624}) than the one observable in MD 3. For the MD 2, the distance between the mass centers is still high to enable a direct interaction between LSKL peptide and KTFR sequence. At the end of the MD 2, the distance keeps increasing, supporting the previous observations, *i.e.* during this simulation, LSKL peptide was not able to reach a stable position at ADAMTS1 surface.

The distance between the mass center of LSKL peptide and the mass center of KTFR sequence plotted along the six supplementary MD simulations with different starting velocities (Figure S3A and Figure S3B) show that these MD simulations converged to the same binding mode characterized by the same non-bonded interactions, which were highlighted in MD 1 and in MD 3 (Table S1). Therefore, these results support the assumption that pose 1 is the most likely binding mode (Figure 4B).

In the MD simulation with pose 2 as starting structure, the analysis of the evolution of the distance between mass center of LSKL peptide and the mass center of KTFR sequence (Figure 3B) shows that the LSKL peptide is positioned farther than during the three MD simulations starting with the pose 1. This distance appears to fluctuate in the three MD simulations, indicating that the position of LSKL peptide and its conformation are not stable. Moreover, the dynamical behaviors of the complex are different along the trajectories and no convergent binding mode was reached. These observations suggest that pose 2 does not correspond to a stable mode of interaction between LSKL peptide and KTFR sequence.

Discussion and conclusions

While TGF-β plays an important role in regulating cell homeostasis, disregulation of TGF-β is associated with numerous diseases, including fibrosis and cancer [5]. The accurate control of the activation of the latent form of TGF-β that regulates the release of active TGF-β is therefore important to prevent the disruption of the normal homeostasis. In liver fibrosis, we have shown that the disintegrin ADAMTS1 is upregulated and triggers TGF-β activation through the interaction between ADAMTS1 KTFR sequence and TGF-β LSKL sequence [4]. The ability of LSKL peptide to block *in vivo* the activation of TGF-β [4, 8] induces a rising interest for a more accurate characterization of the interaction between the LSKL sequence and ADAMTS1. Here, in this aim, we have applied experimental and *in silico* approaches to elucidate this interaction at the atomic level.

Through the experimental binding experiments, we have confirmed that recombinant fragments of human ADAMTS1 containing KTFR sequence are still able to bind TGF-β. Moreover, the F1 recombinant fragment has a higher affinity for TGF-β than the F2 recombinant fragment due likely to a structural stabilization by the cysteine-rich domain. Consequently, the choice of the ADAMTS1 model corresponding to the F1 recombinant fragment was supported by these experimental results. As expected, these interactions showed lower affinities than that of thrombonspondin-1, which binds and activates LAP-TGF-β through two binding sites [24].

So far, the experimental structure of ADMTS1 was not solved, but a model of ADAMTS1 could be built based on template structures of related proteins with reasonable sequence homologies [4]. When no experimental structure is available, a reliable homology model is currently accepted as a sufficient starting point for structure-based drug discovery process [25]. MD simulations suggest that the F1 recombinant fragment model is stable along the trajectories. Moreover, the fact that the KTFR sequence is folded in α-helix leads us to be confident that this region of the model is reliable. In order to predict the conformation and the position of LSKL peptide to the ADAMTS1 surface, molecular docking computations have been done using AutoDock program [18-19], which has been employed successfully for his ability to dock small peptides [15-16]. Two predicted interaction models have been retained based on the binding energy calculated by the scoring function of AutoDock. The stability of these poses has been studied by multiple MD simulations using cumulated simulations time of over 130 ns, which is commonly admitted as sufficient to validate a predicted binding mode [26]. For the lowest energy model, we observe a stable binding mode between LSKL peptide and ADAMTS1

KTFR sequence, characterized by 3 salt bridges and 2 hydrogen bonds (Figure 4B). Overall, without any consideration of the putative region of ADAMTS1 able to interact with the LSKL peptide, our results obtained using *in silico* approaches are consistent with the experimental information previously collected [4, 8].

Our present results provide helpful information to suggest possible chemical modifications for improving potency and specificity, such as mutations combined to the size extension of LSKL peptide or the design of peptidomimetics. Such approach could be duplicated to other proteins of the ADAMTS1 family in order to improve our understanding of the specificity of the interaction between ADAMTS1 and LAP-TGF-β. In the longer term, the identification of potential inhibitors of the interaction between ADAMTS1 and LAP-TGF-β will allow the control of the specific activation of LAP-TGF-β by ADAMTS1 and, consequently, contribute to the reduction of the liver fibrosis.

Conflict of Interest

The authors declare no conflicts of interest.

Acknowledgements:

We would like to thank the University Paris Diderot and INSERM institute for the funding of this work.

References:

1. Egeblad, M.; Werb, Z. New functions for the matrix metalloproteinases in cancer progression. *Nat. Rev. Cancer* **2002**, *2* (3), 161-74.

2. Mochizuki, S.; Okada, Y. ADAMs in cancer cell proliferation and progression. *Cancer Sci.* **2007**, *98* (5), 621-8.

3. Tan Ide, A.; Ricciardelli, C.; Russell, D. L. The metalloproteinase ADAMTS1: a comprehensive review of its role in tumorigenic and metastatic pathways. *Int. J. Cancer* **2013**, *133* (10), 2263-76.

4. Bourd-Boittin, K.; Bonnier, D.; Leyme, A.; Mari, B.; Tuffery, P.; Samson, M.; Ezan, F.; Baffet, G.; Theret, N. Protease profiling of liver fibrosis reveals the ADAM metallopeptidase with thrombospondin type 1 motif, 1 as a central activator of transforming growth factor beta. *Hepatology* **2011**, *54* (6), 2173-84.

5. Ikushima, H.; Miyazono, K. TGFbeta signalling: a complex web in cancer progression. *Nat. Rev. Cancer* **2010**, *10* (6), 415-24.

6. Korpal, M.; Kang, Y. Targeting the transforming growth factor-beta signalling pathway in metastatic cancer. *Eur. J. Cancer* **2010**, *46* (7), 1232-40.

7. Shi, M.; Zhu, J.; Wang, R.; Chen, X.; Mi, L.; Walz, T.; Springer, T. A. Latent TGF-beta structure and activation. *Nature* **2011**, *474* (7351), 343-9.

8. Kondou, H.; Mushiake, S.; Etani, Y.; Miyoshi, Y.; Michigami, T.; Ozono, K. A blocking peptide for transforming growth factor-beta1 activation prevents hepatic fibrosis in vivo. *J. Hepatol.* **2003**, *39* (5), 742-8.

9. Leyme, A.; Bourd-Boittin, K.; Bonnier, D.; Falconer, A.; Arlot-Bonnemains, Y.; Theret, N. Identification of ILK as a new partner of the ADAM12 disintegrin and metalloprotease in cell adhesion and survival. *Mol Biol Cell* **2012**, *23* (17), 3461-72.

10. Brooks, B. R.; Bruccoleri, R. E.; Olafson, B. D.; States, D. J.; Swaminathan, S.; Karplus, M. CHARMM: A program for macromolecular energy, minimization, and dynamics calculations. *J. Comput. Chem.* **1983**, *4* (2), 187-217.

11. Brooks, B. R.; III, C. L. B.; Jr, A. D. M.; Nilsson, L.; Petrella, R. J.; Roux, B.; Won, Y.; Archontis, G.; Bartels, C.; Boresch, S.; Caflisch, A.; Caves, L.; Cui, Q.; Dinner, A. R.; Feig, M.; Fischer, S.; Gao, J.; Hodoscek, M.; Im, W.; Kuczera, K.; Lazaridis, T.; Ma, J.; Ovchinnikov, V.; Paci, E.; Pastor, R. W.; Post, C. B.; Pu, J. Z.; Schaefer, M.; Tidor, B.; Venable, R. M.; Woodcock, H. L.; Wu, X.; Yang, W.; York, D. M.; Karplus, M. CHARMM: The biomolecular simulation program. *J. Comput. Chem.* **2009**, *30* (10), 1545-1614.

12. Berman, H. M.; Westbrook, J.; Feng, Z.; Gilliland, G.; Bhat, T. N.; Weissig, H.; Shindyalov, I. N.; Bourne, P. E. The Protein Data Bank. *Nucleic Acids Res.* **2000**, *28* (1), 235-42.

13. Bernstein, F. C.; Koetzle, T. F.; Williams, G. J.; Meyer, E. F., Jr.; Brice, M. D.; Rodgers, J. R.; Kennard, O.; Shimanouchi, T.; Tasumi, M. The Protein Data Bank: a computer-based archival file for macromolecular structures. *J. Mol. Biol.* **1977**, *112* (3), 535-42.

14. Bas, D. C.; Rogers, D. M.; Jensen, J. H. Very fast prediction and rationalization of pKa values for protein-ligand complexes. *Proteins* **2008**, *73* (3), 765-83.

15. Hetenyi, C.; van der Spoel, D. Efficient docking of peptides to proteins without prior knowledge of the binding site. *Protein Sci.* **2002**, *11* (7), 1729-37.

16. Moroy, G.; Ostuni, A.; Pepe, A.; Tamburro, A. M.; Alix, A. J.; Hery-Huynh, S. A proposed interaction mechanism between elastin-derived peptides and the elastin/laminin receptor-binding domain. *Proteins* **2009**, *76* (2), 461-76.

17. Tubert-Brohman, I.; Sherman, W.; Repasky, M.; Beuming, T. Improved docking of polypeptides with Glide. J. Chem. Inf. Model. 2013, 53 (7), 1689-99.

18. Morris, G. M.; Goodsell, D. S.; Halliday, R. S.; Huey, R.; Hart, W. E.; Belew, R. K.; Olson, A. J. Automated Docking Using a Lamarckian Genetic Algorithm and and Empirical Binding Free Energy Function. *J. Comput. Chem.* **1998**, *19*, 1639–62.

19. Morris, G. M.; Huey, R.; Lindstrom, W.; Belew, R. K.; Goodsell, D. S.; Olson, A. J. Autodock4 and AutoDockTools4: automated docking with selective receptor flexiblity. *J. Comput. Chem.* **2009**, *16*, 2785-91.

20. MacKerell, A. D., Jr.; Feig, M.; Brooks, C. L., 3rd. Improved treatment of the protein backbone in empirical force fields. *J. Am. Chem. Soc.* **2004**, *126* (3), 698-9.

21. MacKerell, A. D.; Bashford, D.; Bellott, M.; Dunbrack, R. L.; Evanseck, J. D.; Field, M. J.; Fischer, S.; Gao, J.; Guo, H.; Ha, S.; Joseph-McCarthy, D.; Kuchnir, L.; Kuczera, K.; Lau, F. T.; Mattos, C.; Michnick, S.; Ngo, T.; Nguyen, D. T.; Prodhom, B.; Reiher, W. E.; Roux, B.; Schlenkrich, M.; Smith, J. C.; Stote, R.; Straub, J.; Watanabe, M.; Wiorkiewicz-Kuczera, J.; Yin, D.; Karplus, M. All-atom empirical potential for molecular modeling and dynamics studies of proteins. *J. Phys. Chem. B* **1998**, *102* (18), 3586-616.

22. Haberthur, U.; Caflisch, A. FACTS: Fast analytical continuum treatment of solvation. *J. Comput. Chem.* **2008**, *29* (5), 701-15.

23. Ryckaert, J.-P.; Ciccotti, G.; Berendsen, H. J. C. Numerical integration of the cartesian equations of motion of a system with constraints: molecular dynamics of n-alkanes. *J. Comput. Phys.* **1977**, *23*, 327–41.

24. Murphy-Ullrich, J. E.; Poczatek, M. Activation of latent TGF-beta by thrombospondin-1: mechanisms and physiology. *Cytokine Growth Factor Rev* **2000**, *11* (1-2), 59-69.

25. Cavasotto, C. N.; Phatak, S. S. Homology modeling in drug discovery: current trends and applications. *Drug Discov. Today* **2009**, *14* (13-14), 676-83.

26. Zhao, H.; Caflisch, A. Molecular dynamics in drug design. *Eur J Med Chem.* **2014**, *91*, 4-14.

Figure captions

Figure 1. Binding experiments between LAP-TGF-β and A) thrombospondin-1, B) F1 recombinant fragment and C) F2 recombinant fragment of human ADAMTS1.

Figure 2. Binding modes of LSKL peptide. A) Cartoon representation of ADAMTS1 (green) with the first binding mode (cyan) and the second one (magenta). KTFR sequence is in red. Detailed connectivities between ADAMTS1 (gray) with residues (colored by atom-type with carbon atoms in green) implicated in non-bonded interactions and LSKL peptide in A) the first binding mode (colored by atom-type with carbon atoms in cyan) or B) in the second energy one

(colored by atom-type with carbon atoms in magenta). Hydrogen atoms have been removed for a better visualization. The figure was prepared using PyMOL (DeLano WL 2002 The. PyMOL Molecular Graphics System, http://www.pymol.org).

Figure 3. Time series of the distance between the mass center of LSKL peptide and the mass center of KFTR sequence during the DM simulations with A) the pose 1 as starting conformation and B) the pose 2 as starting conformation.

Figure 4. Snapshots at the end of the A) MD 1 and the B) MD 2. The detailed connectivities between ADAMTS1 (cartoon representation in gray) with residues (colored by atom-type with carbon atoms in green) implicated in non-bonded interactions and LSKL peptide (colored by atom-type with carbon atoms in cyan). KTFR sequence is in red. Hydrogen atoms have been removed for a better visualization.

Figure 1

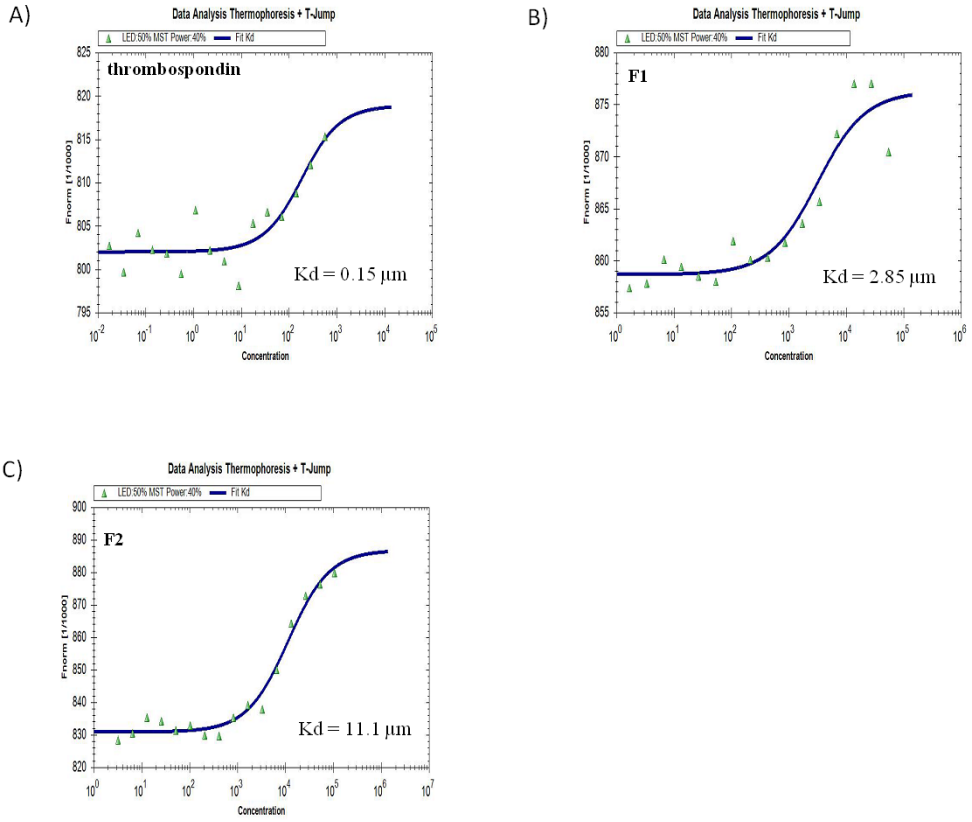

Figure 2

A)

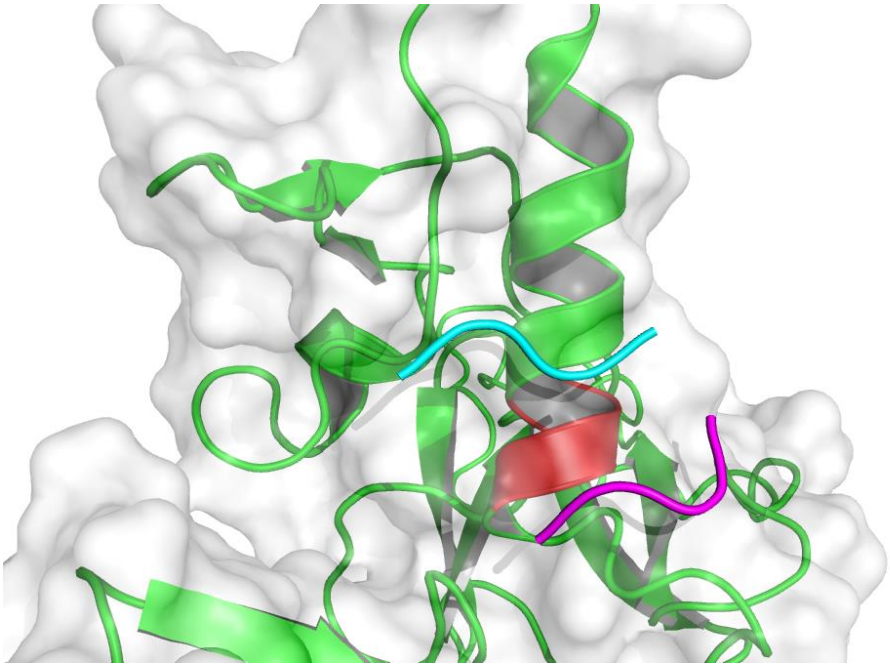

B)

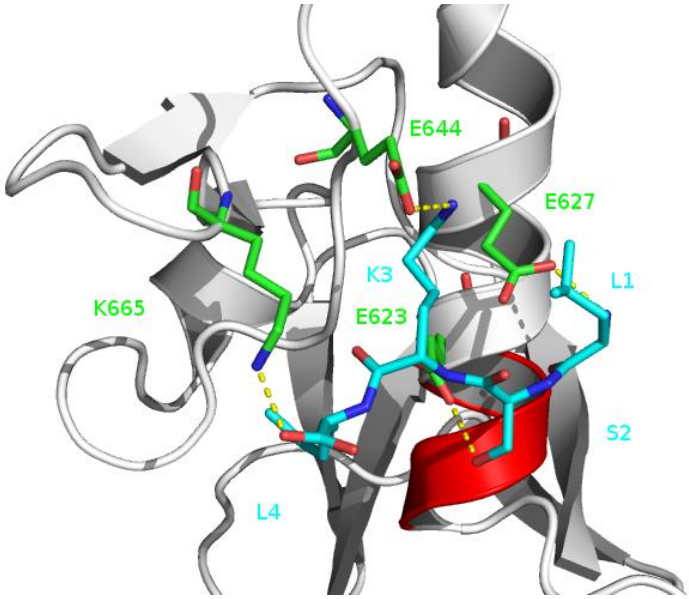

C)

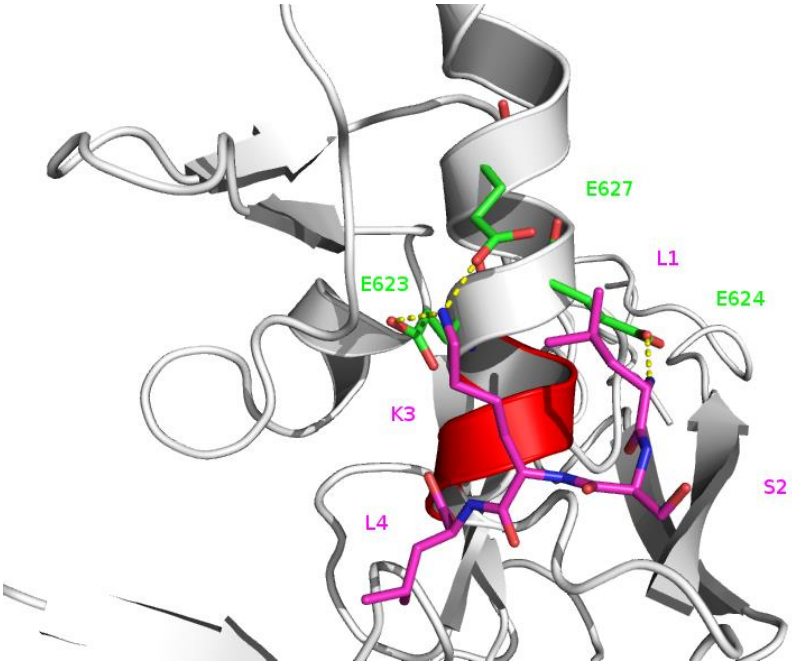

Figure 3

A)

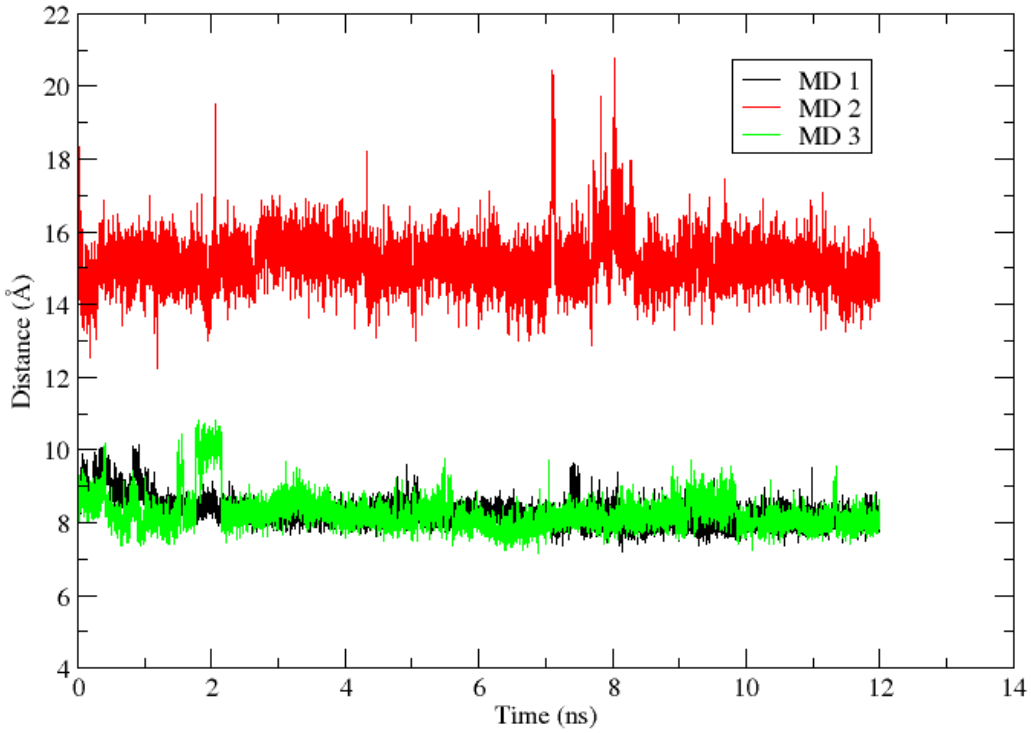

B)

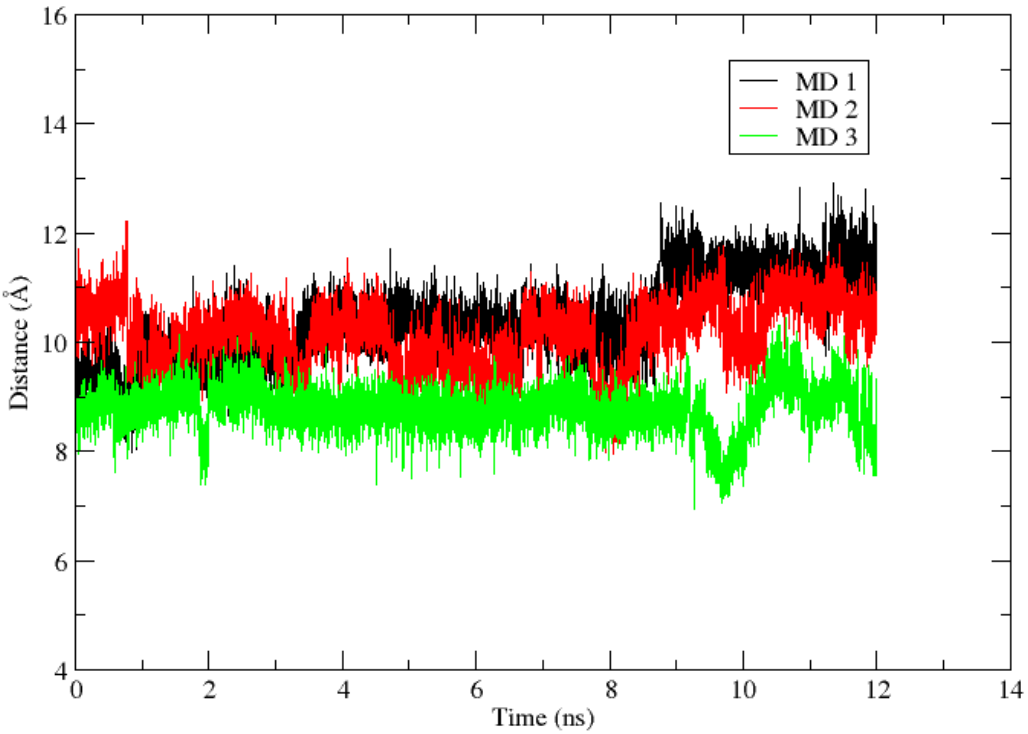

Figure 4

A)

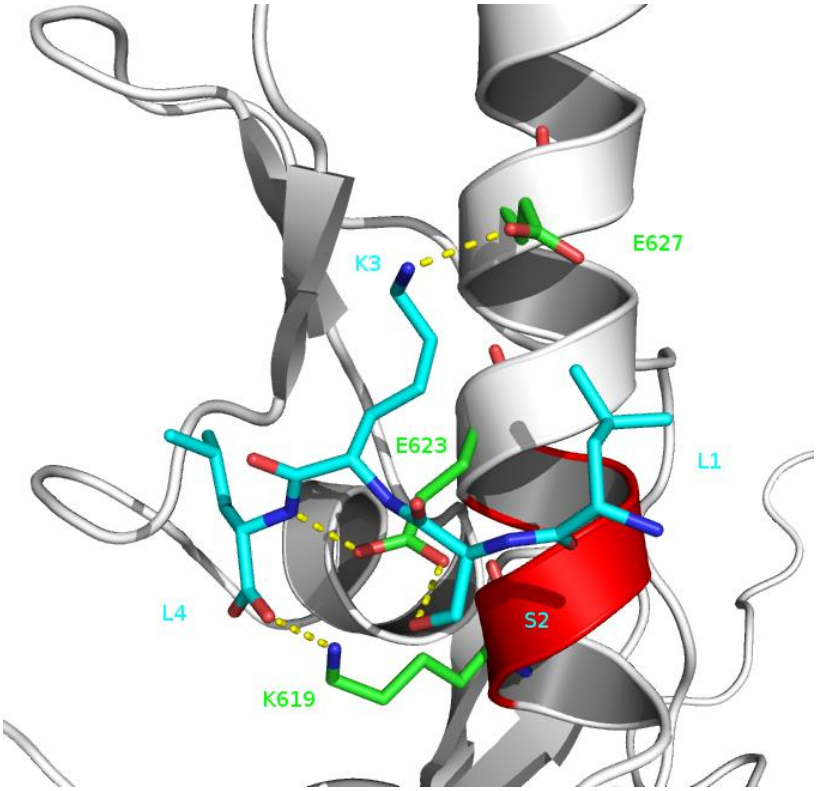

B)